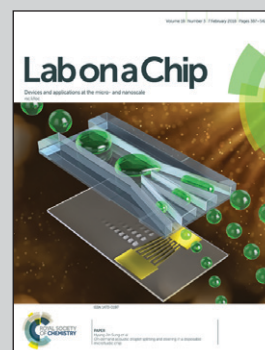


Featuring work from the CAS Key Laboratory of Mechanical Behavior and Design of Materials, Department of Precision Machinery and Precision Instrumentation, Prof. Dong Wu and Prof. Yanlei Hu, University of Science and Technology of China.

Real-time two-photon lithography in controlled flow to create a single-microparticle array and particle-cluster array for optofluidic imaging

A novel method of real-time two-photon lithography in a controlled flow is developed to achieve 100% trapping on a one-bead-to-one-trap basis. In addition, trapping of particle-cluster arrays with a controlled number of particles is also achieved via this method.

As featured in:



See Yanlei Hu, Dong Wu *et al.*,  
*Lab Chip*, 2018, **18**, 442.


 Cite this: *Lab Chip*, 2018, 18, 442

## Real-time two-photon lithography in controlled flow to create a single-microparticle array and particle-cluster array for optofluidic imaging†

 Bing Xu,<sup>a</sup> Yang Shi,<sup>a</sup> Zhaoxin Lao,<sup>a</sup> Jincheng Ni,<sup>a</sup> Guoqiang Li,<sup>ab</sup> Yanlei Hu,<sup>\*a</sup> Jiawen Li,<sup>a</sup> Jiaru Chu,<sup>a</sup> Dong Wu <sup>\*a</sup> and Koji Sugioka<sup>c</sup>

Microarray technology provides an excellent platform for biomedical and biochemical research including basic scientific studies, drug discovery, and diagnostics. Here, we develop a novel method referred to as real-time two-photon lithography in a controlled flow in which femtosecond laser two-photon lithography is performed *in situ* in the sequential mode stopping and flowing the flow of liquid resin containing microparticles to achieve 100% trapping on a one-bead-to-one-trap basis. Polydisperse particles can be all trapped to form a desired array by freely designing trap structures, resulting in an unprecedentedly high capture efficiency of ~100%. No persistent pressure is needed after trapping which reduces the complexity of the system. In addition, trapping of particle-cluster arrays with a controlled number of particles is also achieved *via* this method. The trapped particles inside the microchip are successfully applied as micro-lenses for high quality imaging. The present technology marks an essential step towards a versatile platform for the integration of bead-based assays and paves the way for developing innovative microfluidics, optofluidics, micro-optics and single-cell analysis devices.

 Received 9th October 2017,  
Accepted 1st December 2017

DOI: 10.1039/c7lc01080j

rsc.li/loc

### 1. Introduction

Microarray technology provides an excellent platform for biomedical and biochemical research including quantitative cell biology, drug discovery, and molecular diagnostics due to its capability of simultaneously analyzing large amounts of samples. Microbead arrays are widely used for this technology, since microbead surfaces can be functionalized with various receptors (*e.g.*, antibodies, peptides, DNA, mRNA, enzymes) and their compounds. By utilizing their mobility, functionalized microbeads effectively enrich and separate target analytes on the basis of affinity binding.<sup>1,2</sup>

Microfluidics has received significant attention for microarray applications because of its distinct advantages such as low reagent consumption, easy cell operation, low cost, high integrity, portability and miniaturization.<sup>3–5</sup> To array a large

number of suspended microparticles in a microfluidic chip, a variety of methods have been proposed. Hydrodynamic trap arrays,<sup>6–8</sup> dielectrophoresis (DEP),<sup>9</sup> microwells<sup>10</sup> and acoustic trapping<sup>11</sup> have been demonstrated to successfully form microparticle or cell arrays. In the microwell-based technology, large-scale particle arrays are achieved by size exclusion of randomly seeded particles into the wells, without an external force. Dielectrophoresis uses a non-uniform AC field to manipulate polarized particles in suspension. The use of planar quadrupole trapping or 3D negative dielectrophoretic cages can successfully realize single-microparticle-trap arrays. Acoustic trapping in microfluidic systems commonly employs an ultrasonic standing wave localized in a confined region of a microchannel in which particles are trapped. Compared to the above methods, hydrodynamic trapping is the most common and simplest way to realize cell or particle trapping in a microfluidic system. Trap structures ('U'-shape, 'V'-shape, '\ /'-shape and bypass path) with sizes similar to the average size of cells are firstly fabricated inside a microfluidic channel. Then cells or particles are infused inside the chip to be captured by the trap structures. However, most of the particles are prone to bypass the trap structures because the hydraulic resistance of the microtraps is larger than the free microchannel, which leads to low trapping efficiency (<10%).

A variety of optimized trap designs<sup>12–18</sup> have been proposed to improve the trapping efficiency, but these still do not solve the problem fundamentally. Moreover, a one-bead-

<sup>a</sup> CAS Key Laboratory of Mechanical Behavior and Design of Materials, Department of Precision Machinery and Precision Instrumentation, University of Science and Technology of China, Hefei 230026, China. E-mail: huyi@ustc.edu.cn, dongwu@ustc.edu.cn

<sup>b</sup> Key Laboratory of Testing Technology for Manufacturing Process of Ministry of Education, Southwest University of Science and Technology, Mianyang 621010, China

<sup>c</sup> RIKEN Center for Advanced Photonics, 2-1 Hirosawa, Wako, Saitama 351-0198, Japan

† Electronic supplementary information (ESI) available. See DOI: 10.1039/c7lc01080j

to-one-trap scheme has not yet been achieved due to the randomness in the trapping process.<sup>19–21</sup> Since biological cell types or particles always have polydisperse distributions, the particles with a particular size may escape from the trap arrays with a larger size. The escape of the target particles may result in loss of some important information. Thus it is highly demanded to fabricate a trap array in which the size and geometry can be instantaneously tuned<sup>22,23</sup> to trap all individual particles or cells in order to not miss important information. Such an instantaneously size- and geometry-tuned trap array which can selectively trap target particles while releasing non-target ones further increases the demand for high performance microarray technology.<sup>24</sup> For example, in circulating tumor cell (CTC) research, CTCs in human blood are needed to be selectively captured while releasing blood cells. In conventional methods, before performing cell- and bead-based assays, the mixed sample always needs to be purified by using filters or sorters to remove the non-target particles.<sup>25</sup> Moreover, in a conventional hydrodynamic trap system, a constant pressure is always needed to hold the trapped particles, otherwise the already captured particles may escape. Additionally, simultaneous trapping of multiple cells or particle clusters with a controlled number (more than 2) is highly in demand, since it enables the formation of multi-nucleated cells for studying muscle cell fusion or dynamically monitoring biochemical processes *via* the interaction of engineered particles. However, controlled trapping of multiple cells or particles cannot be achieved by conventional hydrodynamic trap arrays.<sup>26,27</sup>

To address the above problems, we propose a novel real-time two-photon-lithography<sup>28</sup> in controlled flow (TPL-CF) method to achieve reliable trapping on a one-bead-to-one-trap basis. It consists of four steps: 1, the flow of liquid resin containing target particles is stopped to fill a microfluidic chip; 2, pillars are quickly polymerized around target particles to fix the particles; 3, to trap target particles separated from clusters and multiple-particle clusters, the flowing and stopping of liquid are repeated until the target samples are captured; 4, the polymerized resin pillar structures are developed to exchange the solution for the following studies. A CCD camera is used to recognize the target and non-target particles for selective trapping. The sizes and geometries of trap structures can be programmably tuned and then instantaneously fabricated (real-time two-photon lithography) to ensure 100% trapping efficiency. Particles with different sizes, shapes or constituents can be trapped by freely designing trap structures. We examine the critical experimental parameters of the real-time traps including the laser power, particle density, trap size and liquid viscosity. After optimizing these parameters, single-particle and cluster-arrays with controlled numbers and geometries are achieved successfully. Finally, the cluster arrays with different patterns are applied to form microlens arrays for high quality imaging. We envision that this TPL-CF method will find a wide range of applications including microparticle trapping, single cell analysis, new-style optofluidic microlenses for imaging and cell counting.

## 2. Results and discussion

### 2.1 TPL-CF fabrication system

TPL-CF is a real-time fabrication system which performs femto-second laser direct writing two-photon lithography in a PDMS-glass hybrid microfluidic chip, as sketched in Fig. 1a. The microchip is fabricated using PDMS *via* a standard soft lithography technique. The height of the microchannel is designed to be about 24  $\mu\text{m}$  to ensure the capture of only a single particle (20  $\mu\text{m}$ ) by each trap. The PDMS microchannel is then covered with a glass cover slide. The microchannel is connected to a single inlet and also a single outlet, facilitating easy operation. Silica particles (20  $\mu\text{m}$  in diameter) are firstly mixed with a liquid photocurable resin IPL. Then the mixed solution is injected into the microchip from the inlet. The liquid flow is then stopped within 500 ms, so that particles also come to rest. Then, the femtosecond laser is irradiated around the targeted particles to create the trapping pillars. Finally, the laser-exposed resin is developed by washing away the unexposed regions by using alcohol solution. In order to realize fast trapping of individual target particles, the femtosecond laser focused *via* a 50 $\times$  objective lens (NA = 0.8) is scanned from the surface of the glass slide to the ceiling of the PDMS channel with a laser scanning step of 2.4  $\mu\text{m}$ .<sup>29</sup> The formation of multiple pillars around the particle ensures the robustness of the trap.

The four-pillar trap structure can be fabricated in 400 ms (Video S1†) in total which involves a time interval of 10 ms for moving the fabrication positions from one step to the next (Fig. 1b and c). Fig. 1d shows the optical microscopy images of each step in the TPL-CF fabrication process. Reverse and positive flows are used to test whether the particle is adhered to the pillars or not, which verifies that the trapped particles are not damaged by the laser fabrication (Fig. 1e). Six- or eight-pillar traps (Video S2†) can also be used to trap individual particles. Fig. 1f and g and Fig. S1† show the SEM images of the four and eight pillars trapping a 20  $\mu\text{m}$  SiO<sub>2</sub> microparticle. Smaller particles (10  $\mu\text{m}$  silica particles) can also be trapped. The smallest particles which can be successfully trapped are 2.5  $\mu\text{m}$  in diameter. Janus particles and particles with a variety of shapes (Fig. 1h and S2†) such as arrows, ellipses, hearts, 'C', 'E', springs and so on can also be trapped by the TPL-CF method. Two or more particles can also be trapped in identical structures simultaneously (Fig. S2†). The photo of an overall view of the microfluidic chip is shown in Fig. 1i.

### 2.2 Parameter investigations of the TPL-CF system

Fig. 2 shows the key experimental parameters studied for the novel single-trapping method. Indeed, the laser power is a dominant factor to determine the diameter of the pillars. As is known, a larger power can create a larger pillar. A longer exposure time can also create thicker pillars.<sup>30</sup> Fig. 2a demonstrates the relationship between the exposure time and pillar size under different laser powers. It can be clearly seen that 300 or 400 mW are suitable for the successful trapping of the targeted particles when the exposure time is 10 ms. In order to further reduce the fabrication time, a larger power



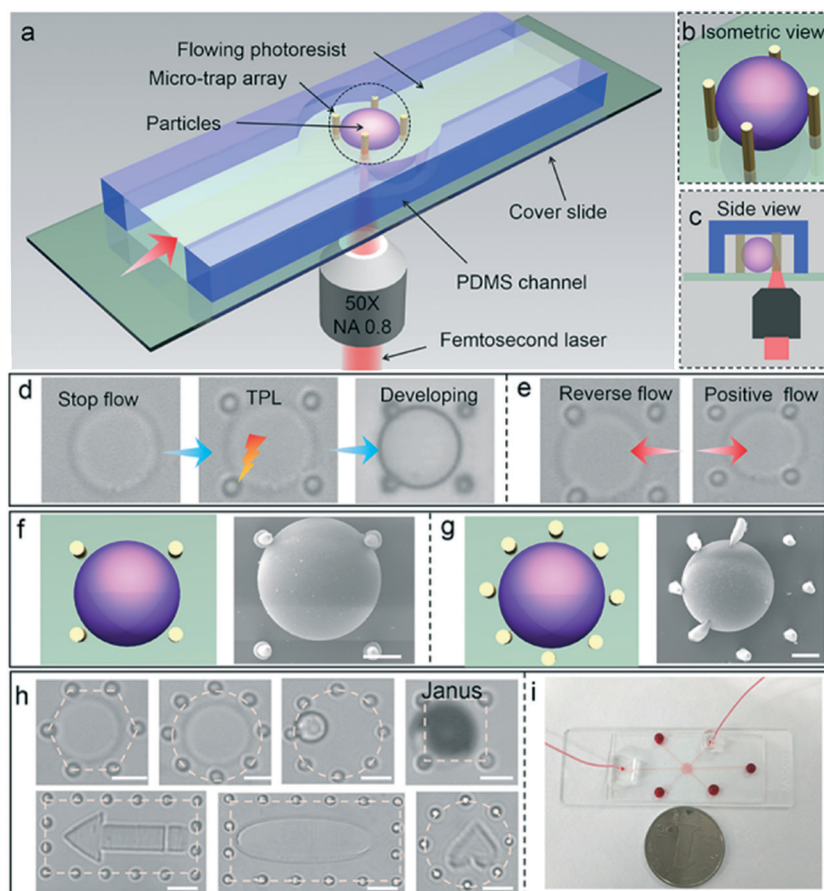


**Fig. 1** TPL-CF real-time single-particle trap. a) The TPL-CF real-time fabrication system in which femtosecond laser two-photon lithography is carried out in a microfluidic chip. b) and c) The isometric and side view images of a trapped particle. d) The real-time trapping procedure: stopping the flow, two-photon lithography to trap the particles, and development to exchange the liquid. e) The trapped particles can move freely inside the trap. f) and g) Schematics and SEM images of the four-pillar trap and eight-pillar trap, respectively. h) The trapping pillars with different numbers and geometries to capture particles of different shapes and constituents. i) Optical microscopy image of the overall view of the microfluidic chip. The scale bars are all 10  $\mu\text{m}$ .

(500 mW) and lower exposure time (1 ms) are adopted. When the laser power reaches 500 mW, a longer exposure time such as 5 or 10 ms leads to the adhesion of the particles to the pillars, resulting in damage to the target particles. A smaller laser power (100 mW) cannot create pillars when the exposure time is 10 ms or shorter. After washing away the liquid resin with alcohol (Fig. S3<sup>†</sup>), the flow speed of a liquid as fast as 10 mL min<sup>-1</sup> didn't collapse the pillars which further proves the stability of the trapping pillars. A single-trapping pillar can be produced with a throughput of about 9000 h<sup>-1</sup> (Table S1<sup>†</sup>) without considering the time for stopping the particles when the laser power is 300 mW and the exposure time is 10 ms. The throughput can be further improved to be 90 000 h<sup>-1</sup> at a larger power and lower exposure time (e.g. 500 mW, 1 ms). To further improve the throughput, multiple foci generated by a spatial light modulator (SLM) can be used to fabricate the pillars (Fig. S4<sup>†</sup>). For example, using a programmable hologram with the help of the GS algorithm, 4 foci can be used to simultaneously produce four-pillar traps, which realize a throughput of 360 000 h<sup>-1</sup> (Table S1<sup>†</sup>). Indeed, this throughput is sufficient for most bead-based analyses.

Conventional trap arrays can only capture a single particle while they cannot trap a single particle separated from clusters consisting of two or more particles. The present TPL-CF method can achieve particle separation from clusters and trap the separated particles. Fig. S5<sup>†</sup> demonstrates the trapping of each particle from clusters consisting of two particles in a one-bead-to-one-trap manner. Firstly, we stop the liquid flow containing clusters and only one particle in the cluster is trapped without damaging any particles; then, the two particles are separated *via* a gentle positive flow; after that, we stop the liquid again and trap the second particle (Fig. S6<sup>†</sup>). It needs to be highlighted that the clusters cannot be trapped in a one-bead-to-one-trap manner by other previous methods. Since the distribution of the particle positions in the microchip is random, the sticking of particles to walls often occurs which also cannot be trapped by conventional hydrodynamic trapping methods while the TPL-CF method can trap these targets easily (Fig. S5<sup>†</sup>). We also investigate the influence of particle density on the single-trapping efficiency (Fig. 2b). The single-trapping efficiency can reach 100% under a suitable particle density (0–30 000 ml<sup>-1</sup>). When the particle density

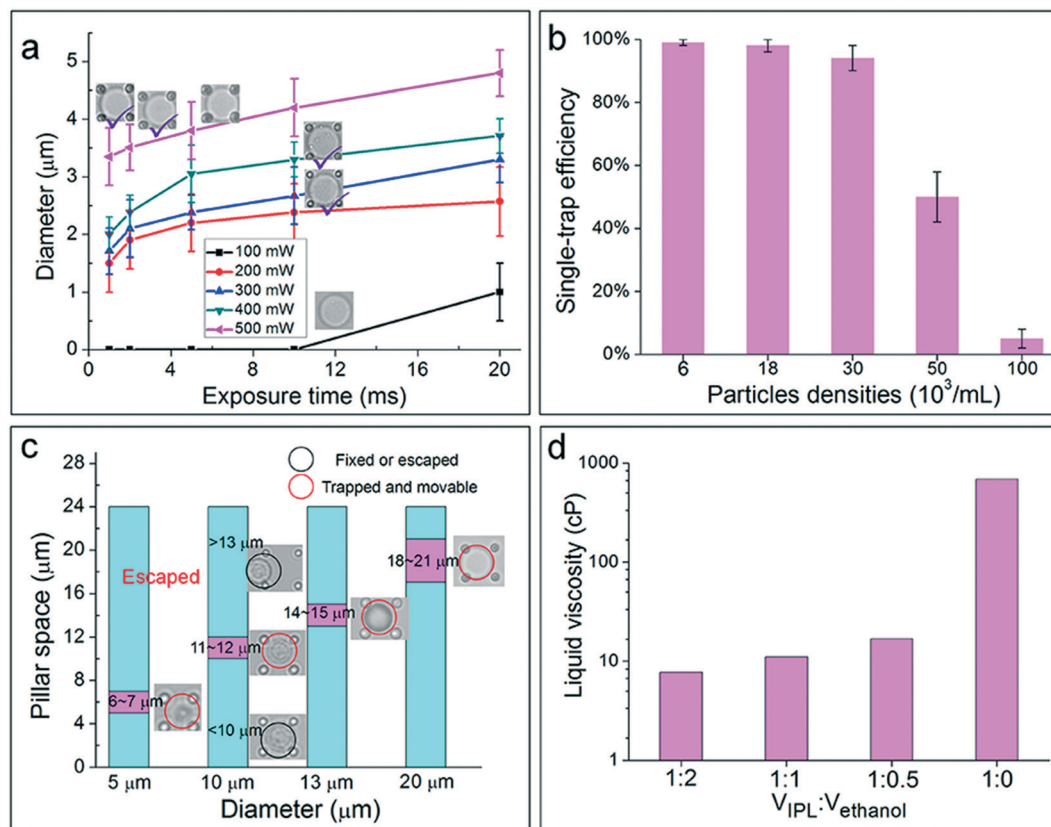


**Fig. 2** Parameter investigations for the fabrication of the TPL-CF trap system. a) Dependence of the pillar diameter on the exposure time for different laser powers. b) The relationship between particle density and single-trapping efficiency. c) Dependence of suitable space between adjacent pillars on the particle diameter for successful single-trapping. d) The viscosity of liquid resin IPL diluted with ethanol at different ratios.

exceeds 50 000 ml<sup>-1</sup>, the single-trapping efficiency significantly drops due to heavy aggregation of particles which cannot be separated into individual ones. In practical single-cell analysis, the cell densities are not always high which is beneficial for the application of the TPL-CF method in single-cell analysis. Fig. 2c shows that the space between four adjacent pillars also influences the particle trapping results. Spaces from 18 to 21 μm are appropriate for no damage trapping of 20 μm particles, while a smaller space (17 μm) may cause adhesion of the particles to the trapping pillars, and a larger pillar space (22 μm) results in particle escape. The appropriate range of trapping pillar spaces for 13 μm, 10 μm and 5 μm particles is 14–15 μm, 11–12 μm and 6–7 μm, respectively. The trapping pillar spaces have the same trend: a larger space leads to particle escape and a smaller one damages the particles. Additionally, the liquid resin IPL needs to be diluted to adjust its viscosity for easier injection and flow operation. The viscosity of pure IPL is 685 cP, which is difficult for infusion and flowing (Fig. 2d and S6†). Ethanol is added into the liquid IPL to adjust its viscosity because of its lower surface tension and good resolvability in IPL resin. When diluting IPL with 200% ethanol, the viscosity of the liquid mixture is about 7.7 cP. Although the flow can be generated easily in this case, the pillars cannot be fabricated because of the ultra-low concentration of the photoinitiator (Fig. S7†). When diluting IPL with 100% ethanol, the laser produces bubbles due to a cavitation effect<sup>31</sup> which is also not suitable for single-particle trapping. The suitable vol-

ume ratio of IPL and ethanol is 1:0.5 which has a viscosity of 16.8 cP to accommodate both the successful fabrication and the easy liquid flow.

### 2.3 Reliable single-trap arrays

After investigating these experimental parameters, we successfully realize reliable single-trap arrays. The patterns of regular single-trap arrays fabricated *via* the TPL-CF method include rectangular (2 × 2), triangular, line (1 × 3), ‘T’, ‘L’, and ‘⊥’ shapes (Fig. 3a–g). Fig. 3h shows a random distribution of a single-trap array without particles adhering to the pillars. It needs to be highlighted that TPL-CF is superior to conventional trapping methods which can only achieve regular trap patterns such as interlaced arrays and often trap multiple particles or no-particles in one single-trap structure. Random single-trap array design has not yet been realized by previous methods because of its low capture efficiency (<1%) and inability to perform trapping in a one-bead-to-one-trap manner.

In order to achieve one-cell-to-one-trap, biocompatible hydrogels can be employed to provide a survivable liquid micro-environment which may realize single-cell traps and investigate the cellular heterogeneity. For example, polyethylene glycol diacrylate (PEGDA) is an inert biomaterial, which has been used extensively for the encapsulation of a diverse array of cells, and has been used in many areas of biomedical

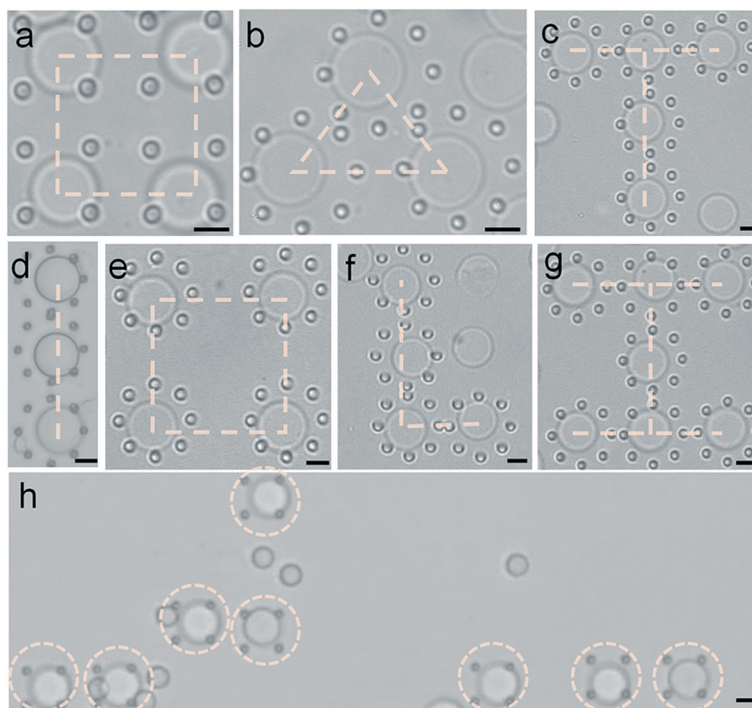


**Fig. 3** Single-trap arrays. a–g) Particle trap patterns in rectangular ( $2 \times 2$ ), triangular, line ( $1 \times 3$ ), ‘T’, ‘L’, and ‘U’ shapes. h) Trapping of randomly distributed particles. Scale bars: 10  $\mu\text{m}$ .

applications. By using suitable concentrations of PEGDA, photoinitiator (e.g. Irgacure 2959), cell culture media and NVP, Panda *et al.* have successfully achieved the fabrication of a large number of cell-laden microgel particles with high cell viability which proves that PEGDA can provide a compatible liquid micro-environment.<sup>32</sup> In addition, commercial bovine serum albumin (BSA), a liquid biomaterial, can also be used for constructing biocompatible microstructures. Sun *et al.* have fabricated protein microlenses by using a femtosecond laser and proved that BSA has excellent biocompatibility.<sup>33</sup> Also, silk fibroin is another biocompatible material which has been successfully introduced in diverse biomedical applications. It has been demonstrated that live bacteria or cells in a silk fibroin liquid-environment can remain alive even if they were close to the laser-processing microareas.<sup>34</sup> With the advantages of high precision, low thermal damage, and noncontact feature, the femtosecond laser one-cell-to-one-trap technique would not induce a significant impact on live bacteria or cells nearby.

#### 2.4 Multi-particle trapping with a controlled number

Nowadays, it is of great importance to enable pairing and clustering of different particles that are related to each other to monitor the interactions taking place in particle clusters. Also, in some biological applications such as cell fusion or cell communication, the target cells need to be paired or to be in contact with each other prior to the following studies.<sup>27</sup> A variety of microfluidic array platforms using several methodologies based on hydrodynamic, electrical, and pneumatic approaches have been reported to this end. Despite the devel-

opment of several technologies such as inkjet and microfluidic chip-based particle dispensing focusing on transferring a controlled number of particles (e.g., microbeads and biological cells) into a reaction chamber or onto a desired site, repeatable and precise control of the number of beads in contact with each other still remains a challenge.<sup>1,2</sup> Here, we demonstrate that the TPL-CF method can achieve real-time trapping of particle clusters with controlled numbers and multiple different components. Fig. 4a is the schematic diagram of the particle cluster trapping with a desired number (Video S3<sup>†</sup>). Firstly, we stop the particle flow and fabricate the multi-pillar trap with one side opening. Then, the liquid flows again to introduce multiple particles into the trap. After the trap is filled with particles, we stop the flow again and seal the trap array with the last pillar at the opening. The whole process is shown in Fig. 4b (a four-particle-cluster trap). Two-, three-, six-, eight-particle clusters can also be trapped by our method. Another advantage of the TPL-CF method is that it can trap multiple particles with different constituents ( $\text{SiO}_2$  particles and Janus particles) in a trap (Fig. 4c), which may find a wider range of applications in cell communication and different particle interactions.

#### 2.5 Particle clusters used as microlenses for imaging

Finally, multi-particle clusters can be used for high quality imaging as microlens arrays. Fig. 5a shows an optical characterization system to test the imaging properties of the particle cluster trapped in the microchip filled with alcohol solution.<sup>35</sup> The intensity distribution on the focal plane of



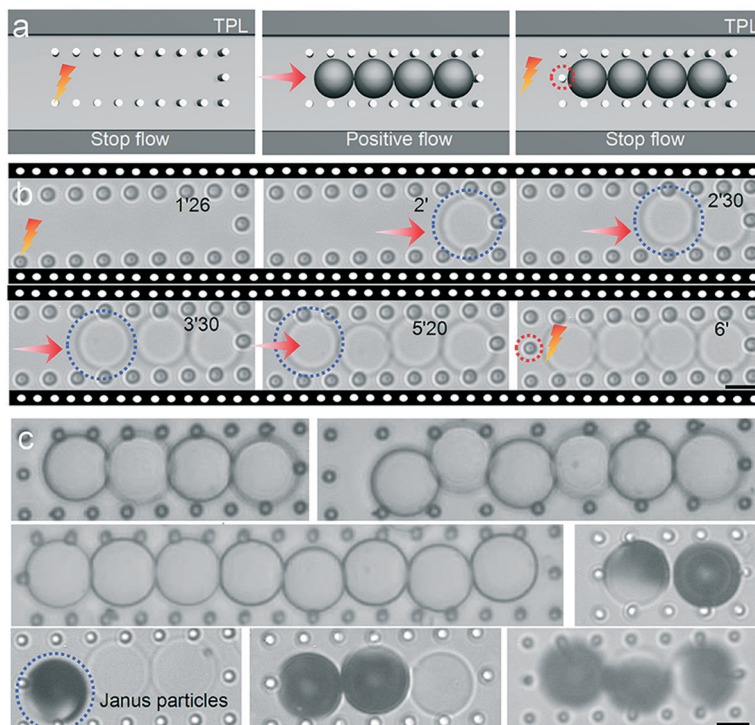


**Fig. 4** Schematic diagram of the multi-particle trapping with a controlled number of particles. a) The trapping procedure, including stopping the flow to create the pillar trap with one opening by two-photon lithography, positive liquid flowing to capture the particles, stopping the flow again and sealing the trap array by forming the last pillar at the opening. b) Sequential photos for the process of 4 particle (20  $\mu\text{m}$ ) trapping inside a multi-pillar trap. c) Trapping of four-, six- and eight-particle clusters and a cluster composed of different particles inside a multi-pillar trap. The scale bars are all 10  $\mu\text{m}$ .

trapped particles can be captured using a CCD camera. Fig. 5b shows the intensity distribution of three trapped particles. The intensity distribution is quite uniform because of the good monodispersity of the particles, which shows that the trapped particles can exhibit excellent performance as microlenses. Different patterns of particle clusters such as rectangles, triangles, ellipses and sinusoidal lines benefitting from our TPL-CF method have been used to image the printed mask (Fig. 5c). The multi-particle cluster patterns may have potential applications in tunable microlenses,<sup>36</sup> bead-based reaction studies<sup>37</sup> and particle self-assembly.<sup>38</sup>

### 3. Conclusion

In conclusion, we have proposed a TPL-CF method to realize reliable single-particle trapping on a one-bead-to-one-trap basis. In contrast to conventional hydrodynamic trapping methods, this novel on-chip single-trap array approach provides several advantages. Firstly, it unprecedentedly improves the capture efficiency to 100%, which thoroughly solves the problem of low capture efficiency for the conventional methods. Secondly, since the TPL-CF method is a real-time and size-tunable processing method, there is no need to pre-design the trap arrays. Thirdly, trapping multiple beads in a trap or no particle trapping is inhibited in our microfluidic chip, and the one-bead-to-one-trap can always be achieved. Fourthly, our method does not need persistent pressure to keep

the trapping which greatly reduces the complexity of the device. Fifthly, particle clusters with controlled particle numbers can be trapped by this system. Finally, a single target particle can be trapped while non-target particles can be released which shows that our method does not need a pre-filter resulting in further reduction of the complexity of the device. We believe that the proposed method is useful in single-cell analysis and provides a new insight into single-particle trapping.

## 4. Methods

### 4.1 Microchip fabrication

The microfluidic devices were fabricated using soft lithography in polydimethylsiloxane (PDMS, Sylgard 184, Dow Corning). Briefly, a layer (24  $\mu\text{m}$  thick) of a photoresist resin, SU-8 2025 (MicroChem, Newton, USA) was spin-coated on a glass slide at 1000 rpm for 20 s and patterned by UV exposure through a photomask designed using AutoCAD software. The PDMS prepolymer was mixed with the crosslinker (Sylgard 184, Dow Corning) at a ratio of 10:1 (w/w). The mixture was then poured onto the glass mold, degassed, and cured at 65  $^{\circ}\text{C}$  overnight. The PDMS substrate was bonded to a glass slide by exposing both surfaces to oxygen plasma.

### 4.2 Microparticle preparation

Silicon dioxide ( $\text{SiO}_2$ ) microspheres with diameters of 5, 10 and 20  $\mu\text{m}$  and polystyrene particles (13  $\mu\text{m}$ ) were bought

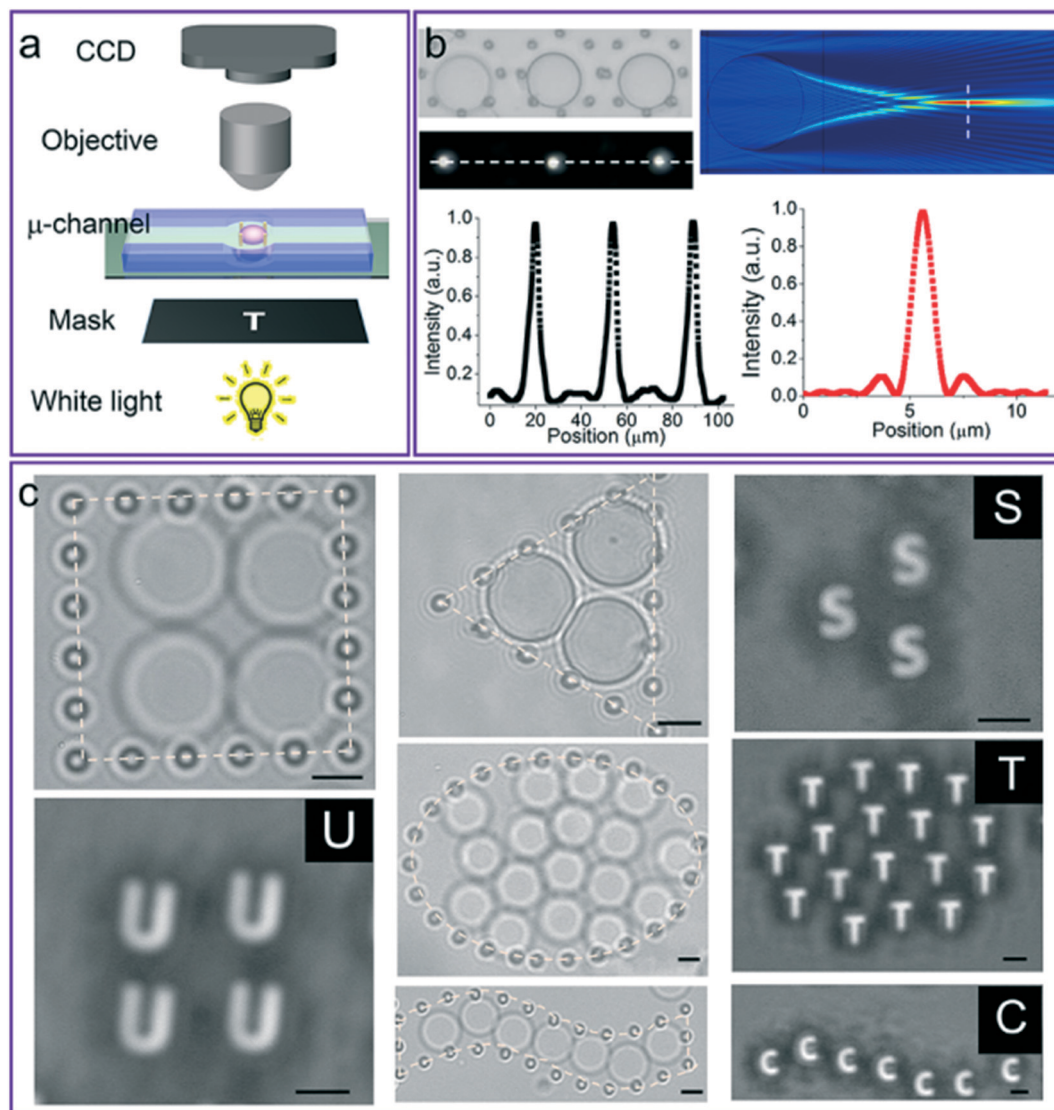


**Fig. 5** Particle cluster used for high quality imaging. a) An optical characterization system to test the imaging properties. b) The intensity distribution produced by three trapped particles. The right image is the optics simulation result obtained by using COMSOL software. c) The imaging results of different patterns of particle clusters such as rectangle, triangle, ellipse and sinusoidal line. All the scale bars are 10  $\mu\text{m}$ .

from Huge Biotech Corp, China.  $\text{SiO}_2$  particles were first dispersed in ethanol. The mixed sample was then spread onto glass slides and dried uniformly to form particle monolayers. For the Janus particles, the  $\text{SiO}_2$  particles were sputter coated with a thin nickel layer (80 nm) using a home-made magnetron sputtering machine. The microparticles with irregular shapes were fabricated by femtosecond laser two-photon polymerization. The microspheres with appropriate concentration were firstly mixed in alcohol solution and then injected into the liquid resin, and finally the mixed liquid was treated in an ultrasonic bath to disperse the particles.

### 4.3 Micropillar trap fabrication

A typical femtosecond laser direct writing system is used for producing real-time micropillar arrays with adjustable sizes, in which a Ti:sapphire laser oscillator (Chameleon Vision-S;

Coherent) is used as the light source, operating at a central wavelength of 800 nm, with a repetition rate of 80 MHz and a pulse duration of 75 fs. A 50 $\times$  objective (Olympus) with N.A. 0.8 is used to focus the laser beam inside the photosensitive material. A commercially available liquid resin (IPL-780, Nanoscribe) without pre-baking and post-baking was used for photopolymerization. The detailed synthesis process is described elsewhere.<sup>39,40</sup> The principal advantage of this material in comparison with other photoresists is that it does not need pre-baking and post-baking. Then, the non-laser-exposed resin remains liquid which can be easily removed with pressure. The viscosity of the liquid resin with different concentrations of alcohol was measured using a rheometer (Physica MCR 301, Anton Paar). A home-made compressed-air flow system was used to precisely control the flowing liquid resin. The liquid resin was injected into PDMS devices at definite pressures. Then the pressure in the inlet was



controlled to be equal to ambient pressure to stop the flow. Four, six or eight robust pillars were fabricated around the particles to capture the target particles. Then, the pressure was added again to implement the next trapping. Rapid alternation with a stoppage time of  $\sim 500$  ms between the flow and stoppage states was achieved with this control system. Here, the flow was considered to be stopped when the bead velocity fell below  $10 \mu\text{m s}^{-1}$ . After multi-particle trapping, the sample was developed in alcohol for 1 day until all of the unpolymerized resin is washed away. After withdrawal from alcohol, water or other liquids can be injected into the micro-channel for the following research.

#### 4.4 Femtosecond laser multifocal fast micropillar trap fabrication

In order to reduce the processing time, a parallel multifocal (4 foci or more foci) processing method was applied using a pre-designed CGH. The 4 spot pattern was firstly designed, and the desired CGH was generated by using a weighted Gerchberg-Saxton (GS) algorithm.<sup>39,40</sup> The intensity of each spot in the desired multifoci pattern was monitored during iteration, and the corresponding weighting factors were employed to update the original target field pattern in the next iterative loop to achieve better uniformity. The CGH with  $1080 \times 1080$  pixels was displayed in the center region of the SLM, which had 256 gray levels corresponding to phase modulation from 0 to  $2\pi$ . After stopping the flow, four robust pillars are simultaneously fabricated around the particles to trap the target particles by multifoci parallel fabrication.

## Conflicts of interest

The authors declare no conflict of interest.

## Acknowledgements

This work is supported by the National Natural Science Foundation of China (No. 51675503, 61475149, 51405464, 61675190, and 51605463), the Fundamental Research Funds for the Central Universities (No. WK2480000002), the China Postdoctoral Science Foundation (No. 2016M590578, 2016M602027), the Chinese Academy of Sciences Instrument Project (YZ201566) and the ‘‘Chinese Thousand Young Talents Program’’.

## References

- H. Kim, I. H. Choi, S. Lee, D. J. Woon, Y. S. Oh, D. Kwon, H. J. Sung, S. Jeon and J. Kim, *Sci. Rep.*, 2017, 7, 46260.
- H. Kim, S. Lee, W. Lee and J. Kim, *Adv. Mater.*, 2017, 1701351.
- T. Thorsen, S. J. Maerkl and S. R. Quake, *Science*, 2002, 298, 580–584.
- G. M. Whitesides, *Nature*, 2006, 442, 368–373.
- E. K. Sackmann, A. L. Fulton and D. J. Beebe, *Nature*, 2014, 507, 181–189.
- D. Di Carlo, L. Y. Wu and L. P. Lee, *Lab Chip*, 2006, 6, 1445–1449.
- L. Y. Lin, Y. S. Chu, J. P. Thiery, C. T. Lim and I. Rodriguez, *Lab Chip*, 2013, 13, 714.
- J. Kim, J. Erath, A. Rodriguez and C. H. Yang, *Lab Chip*, 2014, 14, 2480–2490.
- K. W. Huang, Y. C. Wu, J. A. Lee and P. Y. Chiou, *Lab Chip*, 2013, 13, 3721–3727.
- J. R. Rettig and A. Folch, *Anal. Chem.*, 2005, 77, 5628–5634.
- X. Ding, S.-C. S. Lin, B. Kiraly, H. Yue, S. Li, I.-K. Chiang, J. Shi, S. J. Benkovic and T. J. Huang, *Proc. Natl. Acad. Sci. U. S. A.*, 2012, 109, 11105–11109.
- Q. D. Tran, T. F. Kong, D. Hu and R. H. Lam, *Lab Chip*, 2016, 16, 2813–2819.
- X. X. Xu, P. Sarder, Z. Y. Li and A. Nehorai, *Biomechanics*, 2013, 7, 014112.
- J. Chung, Y.-J. Kim and E. Yoon, *Appl. Phys. Lett.*, 2011, 98, 123701.
- W. H. Tan and S. Takeuchi, *Proc. Natl. Acad. Sci. U. S. A.*, 2007, 104, 1146–1151.
- R. D. Sochol, S. Li, L. P. Lee and L. Lin, *Lab Chip*, 2012, 12, 4168–4177.
- S. Kobel, A. Valero, J. Latt, P. Renaud and M. Lutolf, *Lab Chip*, 2010, 10, 857–863.
- J. P. Frimat, M. Becker, Y. Y. Chiang, U. Marggraf, D. Janasek, J. G. Hengstler, J. Franzke and J. West, *Lab Chip*, 2011, 11, 231–237.
- J. J. Kim, E. Sinkala and A. E. Herr, *Lab Chip*, 2017, 17, 855–863.
- R. Burger, P. Reith, G. Kijanka, V. Akujobi, P. Abgrall and J. Ducrée, *Lab Chip*, 2012, 12, 1289–1295.
- R. Burger, D. Kurzbuch, R. Gorkin, G. Kijanka, M. Glynn, C. McDonagh and J. Ducrée, *Lab Chip*, 2015, 15, 378–381.
- J. P. Beech and J. O. Tegenfeldt, *Lab Chip*, 2008, 8, 657–659.
- W. M. Liu, C. Tian, M. M. Yan, L. Zhao, C. Ma, T. B. Li, J. Xu and J. Y. Wang, *Lab Chip*, 2016, 16, 4106–4120.
- L. Pang, W. M. Liu, C. Tian, J. Xu, T. B. Li, S. W. Chen and J. Y. Wang, *Lab Chip*, 2016, 16, 4612–4620.
- H. Kim, S. Lee, J.-H. Lee and J. Kim, *Lab Chip*, 2015, 15, 4128–4132.
- A. M. Skelley, O. Kirak, H. Suh, R. Jaenisch and J. Voldman, *Nat. Methods*, 2009, 6, 147–152.
- B. Dura, Y. Liu and J. Voldman, Deformability based microfluidic cell pairing and fusion, *Lab Chip*, 2014, 14, 2783–2790.
- S. C. Laza, M. Polo, A. A. Neves, R. Cingolani, A. Camposo and D. Pisignano, *Adv. Mater.*, 2012, 24, 1304–1308.
- Y. L. Hu, Z. X. Lao, B. P. Cumming, D. Wu, J. W. Li, H. Y. Liang, J. R. Chu, W. H. Huang and M. Gu, *Proc. Natl. Acad. Sci. U. S. A.*, 2015, 112, 6876–6881.
- D. Wu, Q. D. Chen, L. G. Niu, J. N. Wang, J. Wang, R. Wang, H. Xia and H. B. Sun, *Lab Chip*, 2009, 9, 2391–2394.
- S.-Y. Park, T.-H. Wu, Y. Chen, M. A. Teitell and P.-Y. Chiou, *Lab Chip*, 2011, 11, 1010–1012.

- 32 P. Panda, S. Ali, E. Lo, B. G. Chung, T. A. Hatton, A. Khademhosseini and P. S. Doyle, *Lab Chip*, 2008, **8**, 1056–1061.
- 33 Y. L. Sun, W. F. Dong, R. Z. Yang, X. Meng, L. Zhang, Q. D. Chen and H. B. Sun, *Angew. Chem., Int. Ed.*, 2012, **51**, 1558–1562.
- 34 Y. L. Sun, Q. Li, S. M. Sun, J. C. Huang, B. Y. Zheng, Q. D. Chen, Z. Z. Shao and H. B. Sun, *Nat. Commun.*, 2015, **6**, 8612.
- 35 D. Wu, S. Z. Wu, L. G. Niu, Q. D. Chen, R. Wang, J. F. Song, H. H. Fang and H. B. Sun, *Appl. Phys. Lett.*, 2010, **97**, 031109.
- 36 Y. C. Seow, S. P. Lim and H. P. Lee, *Lab Chip*, 2012, **12**, 3810.
- 37 T. Tonooka, T. Teshima and S. Takeuchi, *Microfluid. Nanofluid.*, 2013, **14**, 1039.
- 38 Y. Xia, Y. Yin, Y. Lu and J. McLellan, *Adv. Funct. Mater.*, 2003, **13**, 907.
- 39 B. Xu, W. Q. Du, J. W. Li, Y. L. Hu, L. Yang, C. C. Zhang, G. Q. Li, Z. X. Lao, J. C. Ni, J. R. Chu, D. Wu, S. L. Liu and K. Sugioka, *Sci. Rep.*, 2016, **6**, 19989.
- 40 B. Xu, W. J. Hu, W. Q. Du, Y. L. Hu, C. C. Zhang, Z. X. Lao, J. C. Ni, J. W. Li, D. Wu, J. R. Chu and K. Sugioka, *Opt. Express*, 2017, **25**, 16739–16753.